

On Sommerfeld precursor in a Lorentz medium

Adam Ciarkowski

*Institute of Fundamental Technological Research
Polish Academy of Sciences*

Abstract

A one-dimensional electromagnetic problem of Sommerfeld precursor evolution, resulting from a finite rise-time signal excitation in a dispersive Lorentz medium is considered. The effect of the initial signal rate of growth as well as of the medium dumping on the precursor shape and its magnitude is discussed. The analysis applied is based on an approach employing uniform asymptotic expansions. In addition, new approximate formulas are given for the location of the distant saddle points which affect local frequency and dumping of the precursor. The results obtained are illustrated numerically and compared with the results known from the literature.

1 Introduction

Fundamental investigations on EM signal propagation in the Lorentz model of a dispersive medium are due to Sommerfeld [1] and Brillouin [2, 3]. These authors revealed that in addition to the main signal propagating in the medium, two precursors are formed which precede the signal. The front of the fastest (Sommerfeld) precursor propagates in the medium with the velocity of light. The instantaneous oscillation frequencies of the precursors and their local dumping are directly related to the locations in the complex frequency plane of the corresponding saddle points in the integral representation of the signal. Those locations vary with space and time, and are governed by the saddle point equation (SPE) in Eq. (9), requiring that the phase function in the integrand in that representation be stationary. Analysis of the equation shows that there are two pairs of dominant saddle points, the distant and the near ones, responsible for the first (referred to as Sommerfeld) and the second (Brillouin) precursors, respectively. The saddle points in each pair are located symmetrically with respect to the frequency imaginary axis, the fact being related to the causality principle.

Since SPE seems to be not solvable in a closed form, attempts have been made to solve it in an approximate manner. Brillouin's approach [3] consisted in replacing the complex index of refraction in SPE by its expansion in powers of frequency, and then solving the simplified equation for frequency. As a result, a simple, approximate formula was found relating complex frequency to the distance and time coordinates. In the case of the Sommerfeld precursor, the applicability of this map was confined to the vicinity of the front of the precursor. Unfortunately, Brillouin, having at his disposal only a non-uniform asymptotic method, could not effectively describe the front evolution, as it corresponds to coalescence of two distant saddle points at infinity, the case not treatable with the method he used. This deficiency was removed by Bleistein and Handelsman [4] who developed a uniform asymptotic approach that extended the validity of asymptotic considerations to the precursor front.

Recently, the problem of asymptotic analysis of signal propagation in dispersive media has been reexamined by many authors. Extensive research in this field is due to Oughstun and Sherman [5] and Kelbert and Sazonov [6]. In a recent work, [7] Dvorak, Ziolkowski and Felsen offered a new hybrid approach combining both the asymptotic and FFT methods, the former being responsible for extreme parts of the signal frequency spectrum.

In this work we reconsider the asymptotic model of signal propagation in a Lorentz medium, and concentrate on the Sommerfeld precursor. We assume that the Sommerfeld precursor is excited in the Lorentz medium by a sine modulated signal, with its envelope described by a hyperbolic tangent function. Such a representation provides a convenient model for signals with finite rise time. Unlike the Oughstun-Sherman study ([5], Secs. 4.3.4, 7.2.7 and 7.3.7), where the signal envelope was described by an everywhere non-zero smooth function, our initial signal has the form of an abruptly switched modulated sine signal, i.e. it vanishes identically for $t < 0$ and its envelope is non-zero for $t > 0$. At $t = 0$ the derivative of the envelope suffers a step discontinuity. We study the influence of both the medium and the initial signal characteristics, including medium damping δ and signal speed factor β , on the evolution of the Sommerfeld precursor in the medium. In particular, we analyze how the speed factor affects the shape and the magnitude of the precursor excited by both the slow and the fast growing incident signals. We also obtain a simple approximation for the precursor damping factor. Finally, we provide a new approximation to the location of the saddle points, which is more accurate than those known in the literature.

The results obtained here may appear to be useful e.g. in designs employing fast Sommerfeld precursors as signals triggering the electronic devices designed to process the main signal.

2 The propagation problem and its exact solution

We consider the 1D problem of EM signal propagation in a Lorentz medium characterized by the complex index of refraction

$$n(\phi) = \left(1 - \frac{b^2}{\phi^2 - \phi_0^2 + 2i\delta\phi}\right)^{1/2}, \quad (1)$$

where $b^2 = 4\pi Ne^2/m$ is the plasma frequency of the medium, N , e and m are the number of electrons per unit volume, electron charge and its mass, respectively, δ is a damping constant and ϕ_0 is the resonant frequency.

In the plane $z = 0$ of the Cartesian coordinate system $\{x, y, z\}$, the field component $E_x(0, t)$, henceforth denoted by $E_0(t)$, is assumed to be given. It is described by a function, which has the form of a finite rise-time, sine modulated signal

$$E_0(t) = \begin{cases} 0 & t < 0 \\ \tanh(\beta t) \sin(\phi_c t) & t \geq 0. \end{cases} \quad (2)$$

The large positive coefficient β determines how rapidly the signal turns on, and ϕ_c is a fixed carrier frequency. It is also assumed that no EM sources are present at $z \rightarrow \infty$. In [5] a different signal was considered, also employing a tangent hyperbolic function, which, unlike (2), did not vanish for times $t < 0$.

In general, the problem consists in finding the field in the half-space $z > 0$ and for time $t > 0$. The solution to this mixed, initial-boundary value problem for the Maxwell equations takes the form [8]

$$E(z, t) = \frac{1}{2\pi} \int_{ia-\infty}^{ia+\infty} g(\phi; \beta, \phi_c) \exp\left[i\frac{z}{c}\Psi(\phi, \theta)\right] d\phi, \quad (3)$$

where the constant a is greater than the abscissa of absolute convergence for $E_0(t)$. The amplitude and phase functions $g(\phi; \beta, \phi_c)$ and $\Psi(\phi, \theta)$, respectively, are given by

$$g(\phi; \beta, \phi_c) = \frac{1}{2} \left\{ \frac{i}{\beta} \mathcal{B} \left[-\frac{i(\phi - \phi_c)}{2\beta} \right] + \frac{1}{\phi - \phi_c} - \frac{i}{\beta} \mathcal{B} \left[-\frac{i(\phi + \phi_c)}{2\beta} \right] - \frac{1}{\phi + \phi_c} \right\} \quad (4)$$

and

$$\Psi(\phi, \theta) = \phi[n(\phi) - \theta]. \quad (5)$$

The beta function is defined through the psi function as

$$\mathcal{B}(s) = \frac{1}{2} \left[\psi \left(\frac{s+1}{2} \right) - \psi \left(\frac{s}{2} \right) \right]. \quad (6)$$

(For the definition and properties of the psi function see [9], Sec. 6.3.) The beta function is related to the envelope of $E_0(t)$ via the Fourier transformation

$$\int_0^\infty \tanh \beta t e^{i\phi t} dt = \frac{1}{\beta} \mathcal{B} \left(-\frac{i\phi}{2\beta} \right) - \frac{i}{\phi}. \quad (7)$$

Finally,

$$\theta = \frac{ct}{z} \quad (8)$$

is a dimensionless parameter that characterizes a space-time point (z, t) .

In this work we confine our interest to one component of the general solution – the Sommerfeld precursor. A suitable approach to extract this partial field and study its dynamics is to evaluate the integral (3) asymptotically as $z \rightarrow \infty$. At the precursor onset, i.e. as $\theta \rightarrow 1^+$, the distant saddle points in the complex ϕ plane meet at infinity to form a saddle point of infinite order. The valid asymptotic procedure that handles this case is a special instance of application of the general asymptotic theory developed by Bleistein and Handelsman and designed to uniformly evaluate integrals with nearby critical points [10]. (It can also be used in case of more than two coalescing critical points. The case of three critical points: a pole, a branch point and a saddle point was studied in [11].)

Dynamics of the saddle points, essential in asymptotic considerations, is governed by the saddle point equation (SPE)

$$n(\phi) + \phi n'(\phi) - \theta = 0. \quad (9)$$

This equation results from the requirement that the phase (5) should be stationary. It has the form $\theta = f(\phi)$. What we need is the inverse function $\phi = f^{-1}(\theta)$. Approximate solutions to the latter equation were obtained by Brillouin ([3]), Kelbert and Sazonov ([6]) and Oughstun and Sherman ([5]). In Sec. 4 we present another approximate solution, which is more accurate than the solutions known in the literature.

3 Uniform asymptotic representation for the Sommerfeld precursor

The phase function $\Psi(\phi, \theta)$ has the saddle point of infinite order at infinity (see [10], Ch. 9). In this case the classical asymptotic methods break down,

which implies that they cannot be used to describe the precursor behavior at its front (i.e. for $\theta \rightarrow 1^+$). Fortunately, the uniform approach, as proposed in [10], can be effectively used. The term "uniform" means that the resulting asymptotic expansion is valid for any locations of the far saddle points in the ϕ complex plane, including the case where the points (symmetrical with respect to the imaginary axis) coalesce at infinity to create one saddle point of infinite order. As a consequence, the expansion holds for any $\theta \geq 1$, in particular at the precursor front. By using the methods described in [10], Sec. 9.5, we arrive at the following uniform asymptotic representation¹ for the Sommerfeld precursor as $z \rightarrow \infty$:

$$\begin{aligned} E^S(z, t) \sim & -\exp\{-l \operatorname{Im}[\Psi(\phi^+, \theta)]\} \\ & \times \{\operatorname{Re}[G(\phi^+; \beta, \phi_c)] J_1[-l \operatorname{Re}(\Psi(\phi^+, \theta))] \\ & + \operatorname{Im}[G(\phi^+; \beta, \phi_c)] J_2[-l \operatorname{Re}(\Psi(\phi^+, \theta))]\}, \end{aligned} \quad (10)$$

where

$$G(\phi^+; \beta, \phi_c) = \sqrt{\frac{\operatorname{Re}[\Psi(\phi^+, \theta)]}{\Psi_{\phi\phi}(\phi^+, \theta)}} g(\phi^+; \beta, \phi_c), \quad (11)$$

$J_1(\cdot)$ and $J_2(\cdot)$ are Bessel functions of the order 1 and 2, respectively, and $l = z/c$.

In this paper we do not consider possible transition from the precursor to the main signal, which may happen for very high carrier frequency ϕ_c . This occurs when the poles $\phi = \pm\phi_c - 2ik\beta$, $k = 0, 1, 2, \dots$ of the beta function are crossed during deformation of the original contour of integration in (3) to the SDP through $\phi = \phi^\pm$.

A fundamental question that now arises is how the speed parameter β in (2) and the damping parameter δ affect the precursor dynamics in the medium. Below we try to answer this question.

3.1 Dependence of the precursor on β

Let the Lorentz medium considered be described by Brillouin's parameters

$$b = \sqrt{20.0} \times 10^{16} s^{-1}, \quad \phi_0 = 4.0 \times 10^{16} s^{-1}, \quad \delta = 0.28 \times 10^{16} s^{-1} \quad (12)$$

and let us additionally choose

$$\phi_c = 2.0 \times 10^{16} s^{-1}, \quad l = 5.0 \times 10^{-15} s. \quad (13)$$

Assume further that $\beta = 1.0 \times 10^{14} s^{-1}$. The dynamic behavior of the Sommerfeld precursor field corresponding to this data, is shown in Fig. 1.

¹This representation is equivalent, but simplified in form, to that presented in [12]. In [12] the factor 1/4 in Eq.(4.5) should be replaced by 1/8.

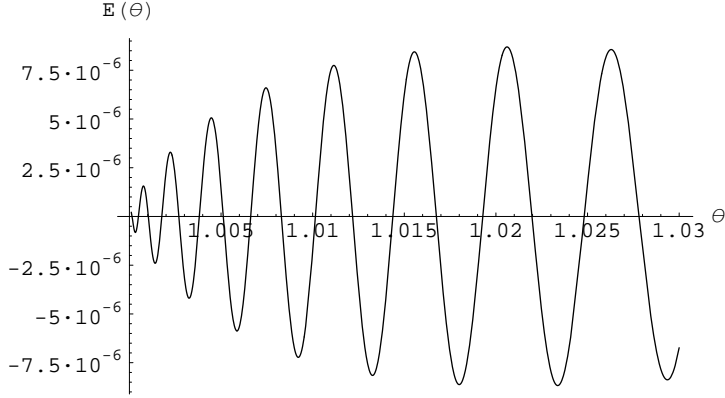


Figure 1: *Dynamic behavior of the Sommerfeld precursor in the Lorentz medium described by Brillouin's parameters. $\phi_c = 2.0 \times 10^{16} s^{-1}$, $l = 5.0 \times 10^{-15} s^{-1}$ and $\beta = 1.0 \times 10^{14} s^{-1}$.*

If now β is increased, by one order or two, it can be shown from (10) that the oscillations in Fig. 1 are increased by the same factor, while the shape of the precursor is preserved. If, however, β takes much higher values, such as $\beta = 1.0 \times 10^{19} s^{-1}$ or more, the precursor shape distinctly changes (see Fig. 2), and the oscillation amplitudes virtually remain at the same, relatively high level as β further increases.

This interesting behavior can be explained by studying properties of the function $G(\phi^+; \beta, \phi_c)$. The plot of $G(\phi^+; \beta, \phi_c)$ as a function of β with fixed remaining arguments is presented in Fig. 3.

The value 1.0001 of the variable θ was chosen what corresponds to the close vicinity of the precursor front (cf. Fig. 1 and Fig. 2). It is seen from the plot that there are three characteristic regions of $G(\phi^+; \beta, \phi_c)$ variation. If for fixed ϕ^+ the parameter β is relatively small then the real part of function $G(\phi^+; \beta, \phi_c)$ is virtually zero and the essential contribution to the precursor is due to its imaginary part. This contribution increases in value with rising β until about $\beta = 4.0 \times 10^{17} s^{-1}$. This is the first region in which the precursor oscillation is described by the Bessel function J_2 . In the second, transitory region, the real part of G grows rapidly, and at about $\beta = 2.0 \times 10^{19} s^{-1}$ it settles down at a virtually constant level. The imaginary part reaches its maximum and then steadily decreases to zero. Here the contribution of the Bessel function J_1 takes over. Finally, in the third region the real part of G remains nearly unchanged and the imaginary part vanishes. Now the contribution of J_1 dominates and that of J_2 is to be neglected. One can verify

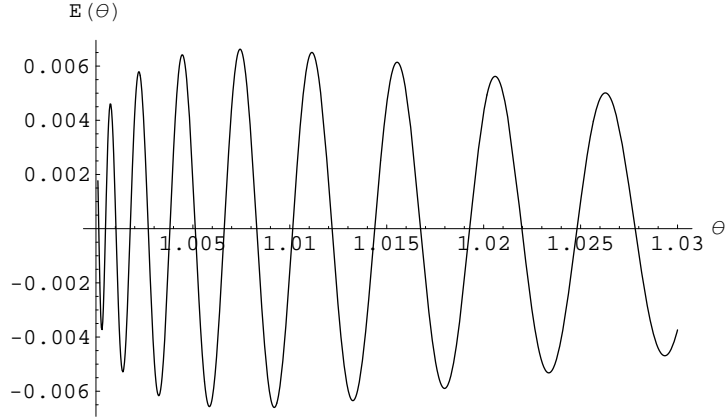


Figure 2: *Dynamic behavior of the Sommerfeld precursor in the Lorentz medium described by Brillouin's parameters. $\phi_c = 2.0 \times 10^{16} s^{-1}$, $l = 5.0 \times 10^{-15} s^{-1}$ and $\beta = 1.0 \times 10^{19} s^{-1}$.*

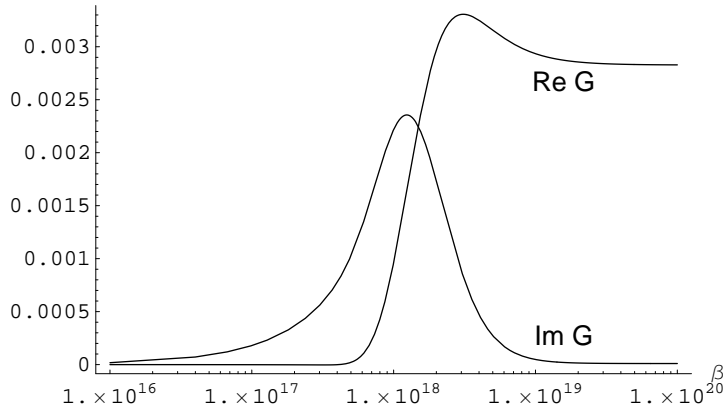


Figure 3: *Dependence of the real (solid line) and imaginary (dashed line) parts of the function $G(\phi^+; \beta, \phi_c)$ on the parameter β . Calculated for $\theta = 1.0001$ and $\phi_c = 2.0 \times 10^{16} s^{-1}$.*

that with increasing θ , the third region broadens, thus pushing the second region in the direction of smaller β .

Below we analyze the precursor behavior in the first and the third regions in more detail. To make the results as simple as possible, we shall employ Brillouin's approximation

$$\phi^+(\theta) \approx \frac{b}{\sqrt{2(\theta-1)}} - 2i\delta. \quad (14)$$

The use of this approximation is justified in the vicinity of the precursor front.

The case of relatively small β

Here, by choosing sufficiently small θ both arguments in functions \mathcal{B} in (4) can be made arbitrarily large. In this case the function G in (11) may be simplified by substituting \mathcal{B} for its asymptotic expression

$$\mathcal{B}(u) = \frac{1}{2u} + \frac{1}{4u^2} + O(u^{-4}), \quad u \rightarrow \pm i\infty, \quad (15)$$

valid also in some sectors centered around the rays $\arg u = \pm i\pi/2$. Then,

$$G(\phi^+; \beta, \phi_c) \sim \sqrt{\frac{\text{Re}(\Psi(\phi^+, \theta))}{\Psi_{\phi\phi}(\phi^+, \theta)}} \cdot \frac{-4i\beta\phi_c}{(\phi^{+2} - \phi_c^2)^2}. \quad (16)$$

If we expand this in fractional powers of $\theta - 1$ and retain the leading terms, we arrive at

$$G(\phi^+; \beta, \phi_c) \sim \frac{48\sqrt{2}\beta\delta\phi_c(\theta-1)^{3/2}}{b^3} - \frac{8i\beta\phi_c(\theta-1)}{b^2}. \quad (17)$$

Since $\delta\sqrt{\theta-1}/b$ is a small quantity, we can safely retain only the imaginary term. We see that $G(\phi^+; \beta, \phi_c)$ is proportional to β . This fact confirms the observed behavior of G in the first region shown in Fig. 3.

Let us now consider the envelope of the Sommerfeld precursor. It is obtained by replacing the Bessel functions in (10) by their envelopes. A good approximation for these envelopes is $\sqrt{2/(\pi x)}$, where x denotes the argument of a Bessel function. Thus, by (10), the envelope of the precursor can be approximated by

$$\begin{aligned} \tilde{E}^S(z, t) &\approx -\exp\{-l \text{Im}[\Psi(\phi^+, \theta)]\} \\ &\times \sqrt{\frac{-2}{\pi l \text{Re}[\Psi(\phi^+, \theta)]}} \{\text{Re}[G(\phi^+; \beta, \phi_c)] + \text{Im}[G(\phi^+; \beta, \phi_c)]\}. \end{aligned} \quad (18)$$

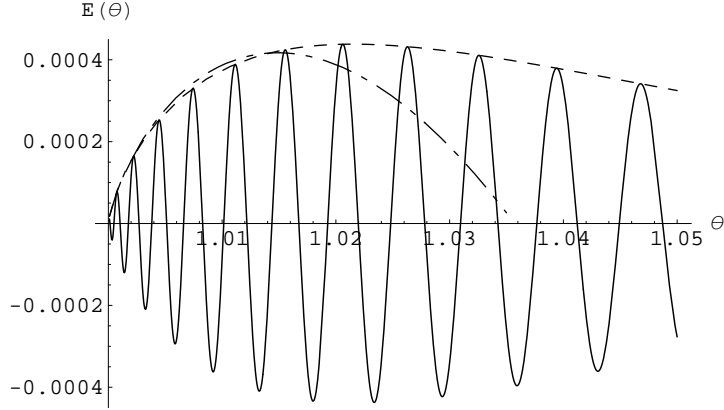


Figure 4: *Sommerfeld precursor, its envelope and the envelope approximation at the precursor front. Calculated for $\beta = 1.0 \times 10^{16} s^{-1}$, $l = 5.0 \times 10^{-15} s$ and $\phi_c = 2.0 \times 10^{16} s^{-1}$.*

Naturally, the notion of the envelope applies here to θ greater than the first extreme of $J_2(x)$, occurring at $x \approx 3.054$. In our case it corresponds to $\theta \approx 1.00009$.

If we are interested in the precursor front only, we can use (14) in (18), replace $G(\phi^+; \beta, \phi_c)$ by RHS of (17), and expand the result in fractional powers of $\theta - 1$. In this manner we arrive at the following approximation of the precursor dynamic behavior at its front:

$$\tilde{E}^S(z, t) \approx \frac{4 \cdot 2^{1/4} \beta \phi_c (\theta - 1)^{3/4} (b - 6\delta \sqrt{2(\theta - 1)}) [1 - 2\delta l (\theta - 1)]}{b^{7/2} \sqrt{\pi l}}. \quad (19)$$

In Fig. 4 an example of the precursor dynamics for $\beta = 1.0 \times 10^{16} s^{-1}$, its envelope as given by (18) and the envelope approximation as given by (19) are shown.

The slope of the envelope is given by

$$\frac{d\tilde{E}^S(z, t)}{d\theta} \approx \frac{2^{1/4} \beta \phi_c \{b [3 - 14\delta (\theta - 1)] + 6\delta \sqrt{2(\theta - 1)} [18\delta (\theta - 1) - 5]\}}{b^{7/2} \sqrt{\pi l} (\theta - 1)^{1/4}}. \quad (20)$$

For sufficiently small θ , the terms proportional to δ can be neglected to yield

$$\frac{d\tilde{E}^S(z, t)}{d\theta} \approx \frac{3 \cdot 2^{1/4} \beta \phi_c}{b^{5/2} \sqrt{\pi l} (\theta - 1)^{1/4}}. \quad (21)$$

It is seen that the slope of the precursor envelope steadily decreases with growing θ .

The case of large β

For finite ϕ^+ and sufficiently large β , the arguments in the functions \mathcal{B} in (4) can be made arbitrarily small. Then the asymptotic expansion is

$$\mathcal{B}(u) = \frac{1}{u} + \ln 2 + \frac{\pi^2 u}{12} + O(u^2), \quad u \rightarrow 0. \quad (22)$$

With its use in (11), the approximation for $G(\phi^+; \beta, \phi_c)$, appropriate for the third region in Fig. 3, follows:

$$G(\phi^+; \beta, \phi_c) \sim \sqrt{\frac{\text{Re}(\Psi(\phi^+, \theta))}{\Psi_{\phi\phi}(\phi^+, \theta)}} \cdot \frac{-\phi_c [24\beta^2 + \pi^2(\phi^{+2} - \phi_c^2)]}{12\beta^2(\phi^{+2} - \phi_c^2)}. \quad (23)$$

Proceeding as in the previous case, we find the following approximation for the envelope of the Sommerfeld precursor

$$\tilde{E}^S(z, t) \approx \frac{[1 - 2\delta l(\theta - 1)] [b^2 \pi^2 (7 + \theta) + 4(\theta - 1) (96\beta^2 + \pi^2 \phi_0^2)] \phi_c}{192 \cdot 2^{1/4} b^{3/2} \sqrt{\pi l} \beta^2 (\theta - 1)^{3/4}}, \quad (24)$$

where minimal θ (here, $\theta \approx 1.00003$) corresponds to the first extreme of $J_1(x)$, occurring at $x \approx 1.841$.

Fig. 5 shows the precursor dynamic behavior for $\beta = 1.0 \times 10^{19} \text{s}^{-1}$, its envelope and the approximation to the envelope as given by (24). Notice that for any finite β there exists a θ , below which the assumption of large β and moderate ϕ^+ is no longer valid. Therefore one should expect that with rising θ , the precursor dynamics may pass through the stages described by the first or/and second regions in Fig. 3, before it reaches the stage characteristic of the third region.

The slope of the precursor front is

$$\begin{aligned} \frac{d\tilde{E}^S(z, t)}{d\theta} \approx & \frac{b^2 \pi^2 \phi_c [\theta - 25 + 2\delta l(3 + 2\theta - 5\theta^2)]}{768 \cdot 2^{1/4} b^{3/2} \sqrt{\pi l} \beta^2 (\theta - 1)^{7/4}} \\ & + \frac{\phi_c (\theta - 1) [1 - 10\delta l(\theta - 1)] (96\beta^2 + \pi^2 \phi_0^2)}{192 \cdot 2^{1/4} b^{3/2} \sqrt{\pi l} \beta^2 (\theta - 1)^{7/4}}. \end{aligned} \quad (25)$$

If terms proportional to the parameter δ are neglected, this expression reduces to

$$\frac{d\tilde{E}^S(z, t)}{d\theta} \approx \frac{\phi_c [b^2 \pi^2 (\theta - 25) + 4(\theta - 1) (96\beta^2 + \pi^2 \phi_0^2)]}{768 \cdot 2^{1/4} b^{3/2} \sqrt{\pi l} \beta^2 (\theta - 1)^{7/4}}. \quad (26)$$

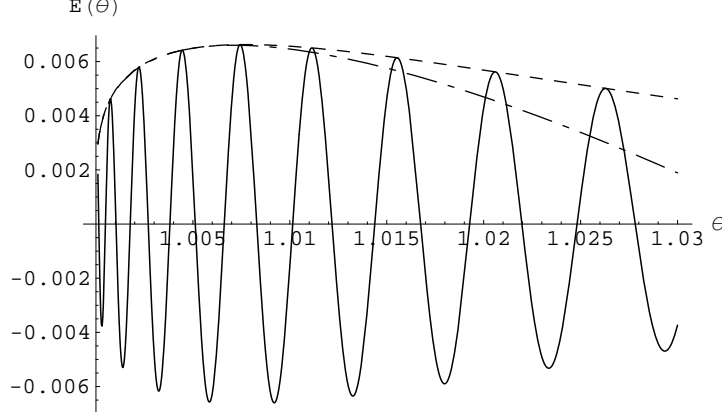


Figure 5: *Sommerfeld precursor, its envelope and the envelope approximation at the precursor front. Calculated for $\beta = 1.0 \times 10^{19} \text{s}^{-1}$, $l = 5.0 \times 10^{-15} \text{s}$ and $\phi_c = 2.0 \times 10^{16} \text{s}^{-1}$.*

As before, the envelope slope decreases with θ . For the parameters used here the rate of the precursor growth is about 16 times higher than in the previous case.

If we formally let β tend to infinity, we obtain from (25)

$$\frac{d\tilde{E}^S(z, t)}{d\theta} \approx \frac{2^{3/4}\phi_c[1 - 10\sqrt{\delta l}(\theta - 1)]}{b^{3/2}\sqrt{\pi l}(\theta - 1)^{3/4}}, \quad (27)$$

which corresponds to the unit-step function envelope in the initial signal.

Finally, let us consider the precursor behavior at the first oscillation, provided β is finite. With the use of (14), (17) and power expansions of the Bessel and exponential functions, we find for $\theta \simeq 1$ (see Fig. 6)

$$\tilde{E}^S(z, t) \approx \beta l \phi_c (\theta - 1)^2 \left(l - \frac{24 \delta}{b^2} \right). \quad (28)$$

This implies that

$$\lim_{\theta \rightarrow 1^+} E^S(z, t) = \lim_{\theta \rightarrow 1^+} \frac{\partial E^S(z, t)}{\partial t} = 0, \quad \lim_{\theta \rightarrow 1^+} \frac{\partial^2 E^S(z, t)}{\partial t^2} \neq 0.$$

On the other hand, we obtain

$$\lim_{t \rightarrow 0} E_0(t) = \lim_{t \rightarrow 0} \frac{dE_0(t)}{dt} = 0, \quad \lim_{t \rightarrow 0} \frac{d^2 E_0(t)}{dt^2} \neq 0.$$

It then follows that the Sommerfeld precursor has the same smoothness properties about $\theta = 1$ as the initial signal (2) has about $t = 0$. This confirms the more general results based on Green's function approach [13] and [14].

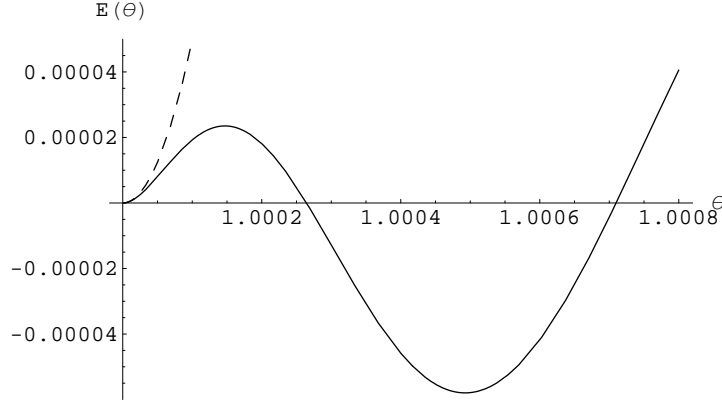


Figure 6: *Onset of the Sommerfeld precursor calculated for $\beta = 1.0 \times 10^{16} \text{s}^{-1}$, $l = 5.0 \times 10^{-15} \text{s}$ and $\phi_c = 2.0 \times 10^{16} \text{s}^{-1}$. The dashed line approximates the precursor growth near $\theta = 1^+$ (Eq. 28).*

3.1.1 Special case

Assume that $\beta \rightarrow \infty$ and $\theta \simeq 1^+$. Then $g(\phi^+; \beta, \phi_c) \approx -2\phi_c \sqrt{2(\theta - 1)} b^{-2}$, and (10) reduces to

$$E^S(z, t) \approx \frac{\phi_c \sqrt{2(\theta - 1)}}{b} J_1(lb \sqrt{2(\theta - 1)}).$$

It is readily seen that this result fully agrees with the representation

$$E^S(z, t) \approx \frac{2\pi}{\tau} \sqrt{\frac{\mathfrak{t}}{\xi}} J_1(2\sqrt{\mathfrak{t}\xi})$$

obtained by Sommerfeld on the grounds of integral considerations and valid for the initial signal described by the Heaviside unit step function ([3], Eq. (33)). Here, we have employed Sommerfeld's notation:

$$\mathfrak{t} = t - \frac{z}{c} \quad \xi = \frac{b^2 z}{2c} \quad \tau = \frac{2\pi}{\phi_c}.$$

3.1.2 A comment on the form of asymptotic representation of the precursor

The form of the asymptotic representation of the Sommerfeld precursor depends on the way $E_0(t)$ behaves at $t \approx 0^+$. First we note that, ([15], Eqs.

(7.128)), the asymptotic behavior of $E_0(t)$ just after it is turned on:

$$E_0(t) \sim \frac{at^r}{r!} \quad \text{as } t \rightarrow 0^+ \quad (29)$$

implies the following asymptotic behavior of g at infinity:

$$g(\phi; \beta, \phi_c) \sim \frac{a}{2\pi} \left(\frac{i}{\phi}\right)^{r+1} \quad \text{as } |\phi| \rightarrow \infty. \quad (30)$$

If the RHS of (30) is used in the basic integral formula describing the signal evolution in a dispersive medium, it appears ([15], Eqs. (7.144)) that in the vicinity of the front, i.e. for $\theta \rightarrow 1^+$, the Sommerfeld precursor dynamics is described by $J_r[b\sqrt{2(\theta-1)z/c}]$. If $\beta \rightarrow \infty$, one has $r = 1$ (which follows from expanding the sine function alone), and the precursor dynamics is described in terms of J_1 . If β is finite, $r = 2$ (see below (28)), and now J_2 describes the precursor development. The orders of the Bessel functions appearing in the uniform asymptotic representation of the precursor are determined from a similar criterion, relating these orders to the behavior of the integrand at infinity. In our case the smallest value of r is 1, which implies the presence of the functions J_1 and J_2 in the asymptotic formula (10).

With increasing θ , the real value of ϕ^+ in the arguments of beta functions in (4) decreases. This results in moving the boundaries between the three characteristic regions of $G(\phi^+; \beta, \phi_c)$ variation with β in the direction of smaller values of β . As a consequence, J_1 describes the precursor behavior not only at $\beta \rightarrow \infty$, but also at finite, sufficiently large values of this parameter (see Fig. 3).

3.2 Decay of the precursor

By expanding the phase function Ψ in terms of powers of δ we obtain

$$\Psi(\phi^+, \theta) = \phi^+ \left(\sqrt{1 - \frac{b^2}{\phi^{+2} - \phi_0^2}} - \theta \right) + \frac{ib^2\phi^{+2}\delta}{(\phi^{+2} - \phi_0^2)^2 \sqrt{1 - \frac{b^2}{\phi^{+2} - \phi_0^2}}} + O(\delta^2). \quad (31)$$

Since the imaginary part of the complex frequency ϕ^+ is small compared to the real part of this frequency, the imaginary part of the phase function Ψ can be approximated with the second term in this expansion.

For θ small, $|\phi^+| \gg \delta$, and we neglect δ in the saddle point equation (9) to arrive at

$$\frac{b^2\phi^{+2}}{(\phi^{+2} - \phi_0^2)^2} + \frac{\phi^{+2} - \phi_1^2}{\phi^{+2} - \phi_0^2} = \theta \sqrt{\frac{\phi^{+2} - \phi_1^2}{\phi^{+2} - \phi_0^2}}. \quad (32)$$

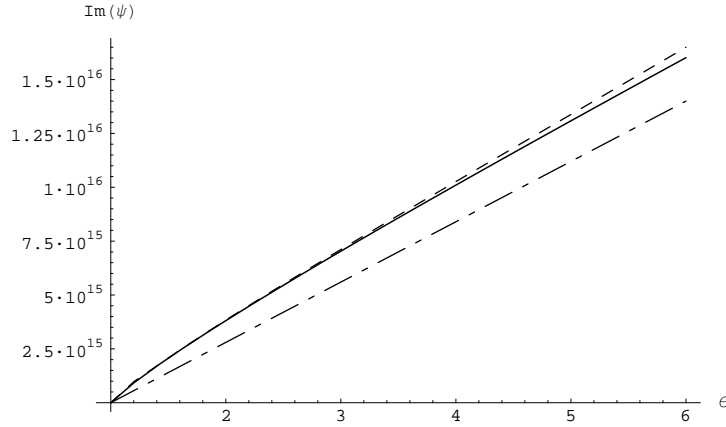


Figure 7: *Comparison of $\text{Im } \Psi(\phi^+, \theta)$ (solid line) with the approximations given in (Eq.31) (dash-dash line) and (Eq.33) (dash-dot line), respectively.*

For θ not too large, the square root at the RHS in this equation, and consequently the second term at its LHS, as well as the square roots in (31), can be approximated by 1. It follows then that the first term in (32), appearing also as a factor in the second term of (31), equals approximately $\theta - 1$. Thus by (31),

$$\text{Im } \Psi(\phi^+, \theta) \approx \delta(\theta - 1). \quad (33)$$

The function $\text{Im}[\Psi(\phi^+, \theta)]$, and its approximations given in (31) and (33) are shown in Fig. 7.

It follows that major cause of the precursor decay is its exponential damping. For low and moderate θ , the exponent determining the rate of decay is approximately equal to $-l\delta(\theta - 1)$. The contribution to precursor decrease due to natural lowering of the oscillation amplitudes in the Bessel functions is of smaller importance.

4 The location of the saddle point $\phi^+(\theta)$

As seen from (10), evolution of the precursor depends on the function $\phi^+(\theta)$ which is a solution to SPE, describing the location of the distant saddle point of (5) in the right complex ϕ half-plane. Since this function does not seem to be expressible in a closed form, approximate formulas for it were found in the literature (Brillouin [3], Oughstun and Sherman [5], and Kelbert and Sazonov [6]). In this section we offer another approximate solution to (9), which is more accurate than the previous ones.

We begin with approximate solution to SPE found in [16] which provides good accuracy for large and medium θ , but fails for θ close to 1. First let us notice that $\phi^+(\theta)$ can be written down in the form

$$\phi^+(\theta) = \sqrt{\phi_0^2 - \delta^2 + \zeta^{-1}(\theta)} - i\delta, \quad (34)$$

where

$$\zeta(\theta) = \frac{1 - n^2(\theta)}{b^2}. \quad (35)$$

The approximation obtained in [16] results from substituting for $n(\theta)$

$$n \approx g - \sqrt{\frac{1}{4a} \left(\frac{\theta}{g} - 2c \right) - g^2}, \quad (36)$$

which leads to approximation of $\zeta(\theta)$, to be denoted by ζ_2 . In (36),

$$g = \frac{1}{2\sqrt{3a}} \sqrt{\frac{2^{-1/3}}{(u + \sqrt{u^2 - v^3})^{1/3}} \left[(u + \sqrt{u^2 - v^3})^{2/3} + v \right] - 2c}, \quad (37)$$

$$u = 2c^3 - 72ace + 27a\theta^2, \quad (38)$$

and

$$v = 2^{2/3}(c^2 - 12ae). \quad (39)$$

The coefficients a , c and e are constant for a given medium and are equal to

$$a = \left[\phi_0^2 - \delta^2 + \frac{i\delta b^2}{\sqrt{\phi_1^2 - \delta^2}} - i\delta\sqrt{\phi_1^2 - \delta^2} - \frac{i\delta b^2[3b^2 + 4(\phi_0^2 - \delta^2)]}{8(\phi_1^2 - \delta^2)^{3/2}} \right] \frac{1}{b^2}, \quad (40)$$

$$c = -\frac{i\delta}{2\sqrt{\phi_1^2 - \delta^2}} - \frac{2}{b^2} \left(\phi_0^2 - \delta^2 - i\delta\sqrt{\phi_1^2 - \delta^2} \right), \quad (41)$$

and

$$e = \frac{\phi_1^2 - \delta^2 - i\delta\sqrt{\phi_1^2 - \delta^2}}{b^2}. \quad (42)$$

We shall denote this approximation by $\phi^+(\theta, \zeta_2)$.

For $\theta \approx 1^+$, i.e. in the vicinity of the precursor front, we find here another approximation. By expressing SPE in terms of the variable ζ we obtain

$$w\zeta - i\delta\sqrt{\zeta}\sqrt{1 + w\zeta} = \frac{\theta n - 1}{b^2\zeta}, \quad (43)$$

where $w = \phi_0^2 - \delta^2$. If $\theta \rightarrow 1^+$ then $\zeta \rightarrow 0$ and this equation can be approximated by

$$w\zeta - i\delta\sqrt{\zeta} = \frac{\theta - 1}{b^2\zeta} - \frac{\theta}{2}. \quad (44)$$

The solution to (44), relevant to our problem can be found by means of the *Mathematica* computer program:

$$\zeta_1 = \frac{1}{2w} \left(u - \frac{q}{2} + \sqrt{2u^2 - 3s - \frac{q^3 - \frac{j}{b^2}q - \frac{8h}{b^2}q}{4u}} \right), \quad (45)$$

where

$$\begin{aligned} q &= \frac{v}{w}, \quad j = b^2\theta^2 - 8(\theta - 1)w, \quad h = -l\theta(\theta - 1), \\ l &= \delta^2 + \theta w, \quad u = \sqrt{s + \frac{q^2}{4} - \frac{j}{6b^2}}, \quad s = \frac{1}{6b^2} \left(\frac{z}{2^{2/3}p} + \frac{p}{2^{4/3}} \right), \\ p &= (r + \sqrt{r^2 - 4z^3})^{1/3}, \quad z = b^4[j^2 - 4 \cdot 12b^2h + 4^2 \cdot 12w^2(\theta - 1)^2], \\ r &= b^6[2j^3 - 12^2b^2jh - 12^2(\theta - 1)^2(8jw^2 - 12b^2l^2 - 12b^2w^2\theta^2)]. \end{aligned} \quad (46)$$

By substituting ζ for ζ_1 in (34), a new approximation of the distant saddle points location is obtained which is valid for θ close to unity. We denote it by $\phi^+(\theta, \zeta_1)$.

The two approximations, $\phi^+(\theta, \zeta_1)$ and $\phi^+(\theta, \zeta_2)$, can now be combined into one formula that provides smooth transition from one approximation to the other. For Brillouin's choice of the medium parameters we choose the transition value of θ to be 1.3. Then the joint approximation can be written down as

$$\begin{aligned} \phi_{SD}(\theta) &= \phi^+(\theta; \zeta_1) \left[H(1.3 - \theta) + \frac{\text{sign}(\theta - 1.3)}{2} \frac{\kappa(\theta - 1.3)}{\kappa(0)} \right] \\ &\quad + \phi^+(\theta; \zeta_2) \left[H(\theta - 1.3) - \frac{\text{sign}(\theta - 1.3)}{2} \frac{\kappa(\theta - 1.3)}{\kappa(0)} \right], \end{aligned} \quad (47)$$

where $H(s)$ is a unit-step function,

$$\kappa(s) = \eta(s + 0.05)\eta(s - 0.05), \quad (48)$$

and

$$\eta(s) = \begin{cases} \exp(-1/s^2), & s > 0, \\ 0, & s \leq 0. \end{cases} \quad (49)$$

Since $\kappa(\theta - 1.3)$ is zero outside the interval $1.25 < \theta < 1.35$, the approximation $\phi_{SD}(\theta)$ equals $\phi^+(\theta, \zeta_1)$ if $\theta < 1.25$, and $\phi^+(\theta, \zeta_2)$ if $\theta > 1.35$. The factors in square brackets in (47) provide smooth transition between the two approximations inside the interval. At $\theta = 1.3$, they are understood in a sense of limits (from the left or from the right), and thus are equal to $1/2$. A different choice of media parameters may require the numerical parameters in (47) and (48) to be modified.

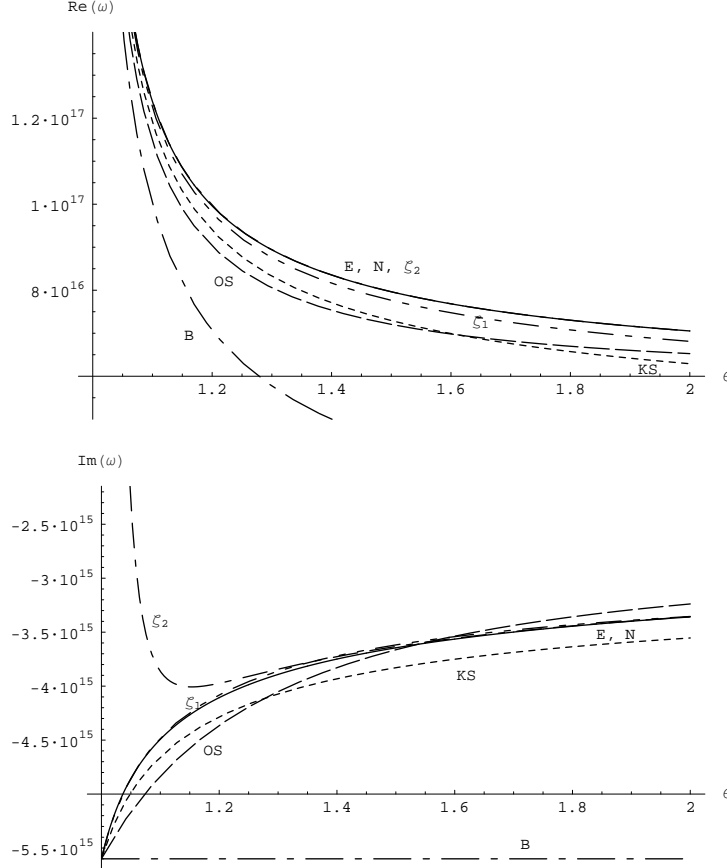


Figure 8: *Real and imaginary parts of various approximate solutions to (Eq.9). Legend: E – exact result (solid line), B – Brillouin’s approximation, OS – Ougstun-Sherman’s approximation, KS – Kelbert-Sazonov’s approximation, N – the result based on (Eq.47), ξ_1 and ξ_2 – the approximations described by $\phi^+(\theta, \xi_1)$ and $\phi^+(\theta, \xi_2)$, respectively.*

The approximation (47) is shown in Fig.8, together with the approximations obtained by Brillouin, Kelbert and Sazonov, Oughstun and Sherman,

and with the partial approximations $\phi^+(\theta; \zeta_1)$ and $\phi^+(\theta; \zeta_2)$. This approximation is not as simple as the first three ones, but may prove to be useful when a higher accuracy is required. Its maximal deviation from the solution of (9) found numerically slightly exceeds 2 percent.

Note that the approximation $\phi^+(\theta; \zeta_2)$ indicates an interesting symmetry between locations of the distant and near saddle points (see [16]). Similar symmetry also follows from the Kelbert-Sazonov approximation.

Acknowledgment

The research presented in this work was partially supported by the State Committee for Scientific Research under grant 8 T11D 020 18.

References

- [1] A. Sommerfeld, "Über die Fortpflanzung des Lichtes in disperdierenden Medien," Ann. Phys. (Lepzig) **44**, 177-202 (1914).
- [2] L. Brillouin, "Über die Fortpflanzung des Lichtes in disperdierenden Medien," Ann. Phys. (Lepzig) **44**, 203-240 (1914).
- [3] L. Brillouin, *Wave Propagation and Group Velocity* (Academic, New York, 1960).
- [4] R.A. Handelsman and N. Bleistein, "Uniform asymptotic expansions of integrals that arise in the analysis of precursors," Arch. Rat. Mech. Anal. **35**, 267-283 (1969).
- [5] K. E. Oughstun and G. C. Sherman, *Electromagnetic Pulse Propagation in Causal Dielectrics*, vol. 16, (Springer, Berlin, 1997).
- [6] M. Kelbert and I. Sazonov, *Pulses and Other Wave Processes in Fluids*, (Kluwer, 1996).
- [7] S.L. Dvorak, R.W. Ziolkowski and L.B. Felsen, "Hybrid analytical-numerical approach for modelling transient wave propagation in Lorentz media," J. Opt. Soc. Am. **A15**, 1241-1255 (1995).
- [8] A. Ciarkowski, "Asymptotic analysis of propagation of a signal with finite rise-time in a dispersive, lossy medium," Arch. Mech., **49**, 877-892 (1997).
- [9] M. Abramowitz and I.A. Stegun, *Handbook of Mathematical Functions*, (National Bureau of Standards, Applied Mathematics Series-55, 1964).

- [10] N. Bleistein and R. A. Handelsman, *Asymptotic Expansions of Integrals* (Holt, Rinehart and Winston, 1975), Ch. 9.
- [11] A. Ciarkowski, "Uniform asymptotic expansion of an integral with a saddle point, a pole and a branch point," Proc. R. Soc. Lond., A **426**, 273-286 (1989).
- [12] A. Ciarkowski, "Improved representation for the first precursor in the Lorentz medium," Eng. Trans., **48**, 43-59 (2000).
- [13] S. Rikte, "Existence, uniqueness, and causality theorems for wave propagation in stratified, temporally dispersive, complex media", SIAM J. Appl. Math., **57**, 1373-1389, (1997).
- [14] S. He, S. Ström and V.H. Weston, *Time Domain Wave-Splittings and Inverse Problems*, (Oxford University Press, 1998).
- [15] J.D. Jackson, *Classical Electrodynamics*, (John Wiley and Sons, Inc., 1975)
- [16] A. Ciarkowski, "Frequency dependence on space-time for electromagnetic propagation in dispersive medium," Arch. Mech., **51**, 33-46 (1999).